

## First-principles supercell studies of the nitrogen impurity in diamond

Steven C. Erwin\* and Warren E. Pickett

*Complex Systems Theory Branch, Condensed Matter and Radiation Sciences Division,  
Naval Research Laboratory, Washington, D.C. 20375-5000*

(Received 13 June 1990)

We have used a first-principles, local-orbital computational scheme to study the electronic structure of a substitutional N donor impurity in cubic diamond. The calculations were carried out in a supercell framework, using three different supercells with increasing impurity-impurity separation. Comparison of the results from all three supercells allows a reliable extrapolation to the isolated-impurity limit; we find that the N impurity level falls at  $E_c - 0.8$  eV, where  $E_c$  is the conduction-band edge. Analysis of the impurity wave function for the three supercells shows that, while the calculated energies indicate a deep donor level, the impurity wave function is nonetheless surprisingly long ranged. The implications of this for the interpretation of recent findings on magnetic multilayers are briefly discussed.

### I. INTRODUCTION

The past several years have been marked by a renewal of interest in the electronic properties of semiconducting diamond. This interest has been stimulated primarily by recent advances in diamond-film growth techniques, which may lead to a variety of technological applications, including low-friction surfaces, wear-resistant coatings, and high-temperature optoelectronic devices. In the past two years, we and our colleagues at the Naval Research Laboratory have been using first-principles local-density approximation (LDA) computational techniques to study theoretically the physical and electronic properties of diamond in order to gain insight into such diverse phenomena as interface bonding and Schottky-barrier formation,<sup>1</sup> and film growth via chemical-vapor deposition.<sup>2</sup> While most of this work has concerned interactions at the diamond surface, equally important are the properties of interior defects, e.g., dopants and vacancies. The present work addresses, from both a physical and computational viewpoint, the problem of a nitrogen substitutional impurity in cubic bulk diamond.

The nitrogen impurity in diamond is not a new problem, and has been treated by several different theoretical techniques. Nonetheless, a complete quantitative description of the impurity energetics and structure is still lacking. Early calculations by Astier, Pottier, and Bourgoïn,<sup>3</sup> using a self-consistent semiempirical method (extended Hückel theory), predicted a deep nitrogen-induced level of  $T_2$  symmetry occurring at 1.3 eV below the diamond conduction-band (CB) edge. The degeneracy of this state was assumed to lead to a Jahn-Teller instability of the neutral impurity, which was purported to explain the experimentally observed trigonal distortion in the nitrogen impurity system. This result was contradicted, however, by Bachelet, Baraff, and Schlüter,<sup>4</sup> who used a self-consistent Green's-function calculation to predict a shallow level (0.15 eV below the CB edge) of  $A_1$  symmetry, and therefore no Jahn-Teller instability. Messmer and Schultz<sup>5</sup> have performed detailed studies for the

analogous case of substitutional N in silicon, using the generalized valence-bond method. They find a stable off-center position for the impurity, driven by local bonding effects argued to arise from strong electron-electron correlation, and have shown elsewhere that the same off-center motion (somewhat diminished in magnitude) is found for N in diamond as well.<sup>6</sup> An unrestricted Hartree-Fock cluster calculation by Sahoo *et al.*<sup>7</sup> also found the nondegenerate  $A_1$  state to lie below the  $T_2$  state, although energy levels were not reported in this work. Nevertheless, the minimum-energy atomic configuration for this cluster showed the nitrogen impurity 0.3 Å away from its substitutional site, along the  $\langle 111 \rangle$  direction. The authors described this effect as purely chemical in origin. Quite recently, this result too was contradicted by Jackson, Pederson, and Harrison,<sup>8</sup> who used an accurate first-principles LDA cluster method to search for global and local minima in the total energy. They found a bound state in the gap of  $A_1$  symmetry, with a level at 0.75 eV below the diamond CB. With the positions of the surrounding atoms fixed at their bulk values, no evidence was found for off-center distortion of the N impurity atom. Finally, a recent 32-atom supercell calculation by Kajihara, Antonelli, and Bernholc<sup>9</sup> found a deep state, of  $A_1$  symmetry, bound by 1.2 eV, and atomic distortion that varied with supercell size and  $k$ -point sampling.

Some of the discrepancies listed above have been explained. In particular, the extended Hückel results have been shown<sup>10,11</sup> to be very sensitive to both the interaction parameters and to the quality of the fit to the diamond CB. However, although a consensus now appears to exist on the  $A_1$  symmetry of the lowest energy gap state, the exact position of this level in the gap is still a matter of some controversy. Also unresolved is the issue of the experimentally observed off-center position of the nitrogen impurity atom: since a Jahn-Teller mechanism does not seem to be driving the instability, what alternative explanation is there?

In the present work, we do not address this last ques-

tion, but rather focus on several other issues that seem to have been neglected. Since clusters are presently limited by available computing resources to two or three shells of carbon atoms, we have decided to approach the problem from a different limit. By using a supercell formalism and periodic boundary conditions, we avoid the problems of surface reconstruction, passivation, and impurity-surface interaction, in exchange for the (possibly) less severe problem of impurity-impurity interaction. We expect this approach to suffer less from size effects because the impurity-impurity distance in a supercell calculation is twice the impurity-surface distance in a cluster calculation of comparable size. One of our primary concerns will be the convergence of results as a function of supercell size (or, equivalently, as a function of impurity separation). Also of interest will be the comparison between our supercell results and the cluster results of Jackson *et al.*<sup>8</sup> Such a comparison will be particularly meaningful because both calculations used a first-principles, full-potential LDA approach, the same basis set (linear combination of atomic orbitals), expanded on the same set of Gaussian functions, and the same interatomic spacing.

The organization of this paper is as follows. In Sec. II, we briefly describe our computational method and the relevant numerical details. Results for the supercell calculations on the C:N system are described in Sec. III and are briefly compared with those of Jackson *et al.*,<sup>8</sup> Bachellet *et al.*,<sup>4</sup> and Kajihara *et al.*<sup>9</sup> In Sec. IV we provide some concluding remarks.

## II. COMPUTATIONAL METHOD

Three separate calculations were carried out for the C:N impurity system, using supercells of eight, 16, and 54 atoms, in order to study the convergence of the impurity-induced energy levels and wave functions as a function of impurity separation. The eight-atom supercell used a simple cubic unit cell, while the 16- and 54-atom supercells were formed from the doubled and tripled two-atom diamond unit cell, respectively. By placing the nitrogen impurity atom at the origin, and carbon atoms (in the diamond configuration) at all the remaining sites in the unit cell, full tetrahedral symmetry of the impurity atom was retained for all three systems. No relaxation was allowed, a reasonable starting assumption in view of the similar tetrahedral covalent radii, 0.70 and 0.77 Å for N and C, respectively. The resulting impurity-impurity separation  $D$ , supercell volume  $\Omega$ , and the number of bonds separating nearest-neighbor impurities  $N_b$ , are listed in Table I for the three supercells.

TABLE I. Various measures of supercell size. Notation:  $N$ , number of atoms per cell;  $D$ , impurity-impurity separation (Å);  $\Omega$ , supercell volume (Å<sup>3</sup>);  $N_b$ , number of bonds between nearest-neighbor impurities.

	C <sub>7</sub> :N	C <sub>15</sub> :N	C <sub>53</sub> :N
$N$	8	16	54
$D$	3.6	5.0	7.6
$\Omega$	45.4	90.8	306.4
$N_b$	4	4	6

These quantities are various geometric measures of the degree to which each supercell approximates the limiting case of an isolated impurity atom. Of course, the true test of sufficient impurity separation is the convergence of the self-consistent electronic structure, which we will present in Sec. III.

All calculations were carried out within the local-density approximation (LDA), using the Hedin-Lundqvist parametrization<sup>12</sup> of the exchange-correlation potential. A recently developed, first-principles, general-potential local-orbital method<sup>13</sup> was used with a linear combination of atomic orbitals (LCAO) framework and Gaussian-orbital basis set. This method has been extensively tested on the elemental diamond, elemental vanadium, and a diamond-nickel (001) ideal interface, and has been shown to give results virtually indistinguishable from those given by state-of-the-art linear-augmented-plane-wave (LAPW) calculations.

Details of the method can be found in Ref. 13, and so we give here only a brief synopsis. The basis functions are wave-vector-dependent combinations of atomic orbitals and bare Gaussian functions, constructed so as to satisfy the requirement of Bloch periodicity:

$$b_{\gamma j}(\mathbf{k}, \mathbf{r}) = N^{-1/2} \sum_{\mathbf{v}} \exp[i\mathbf{k} \cdot (\mathbf{R}_{\mathbf{v}} + \mathbf{T}_{\gamma})] \phi_{\gamma j}(\mathbf{r} - \mathbf{R}_{\mathbf{v}} - \mathbf{T}_{\gamma}). \quad (1)$$

Here,  $\gamma$  denotes the atom found at position  $\mathbf{T}_{\gamma}$  within the unit cell,  $j$  denotes the atomic orbital, and the  $\mathbf{R}_{\mathbf{v}}$  are the Bravais-lattice vectors. The functions  $\phi(\mathbf{r})$  are expanded on a set of Gaussian orbitals, so that all matrix elements of the overlap and kinetic-energy operators can be calculated analytically.<sup>14</sup> By similarly expressing the one-electron effective potential as a sum of Gaussian functions (via a least-squares fitting procedure), all matrix elements of the potential-energy operator can also be calculated analytically or in terms of the error function.<sup>14</sup> The one-electron potential is, of course, a sum of Coulomb and exchange-correlation potentials. To compute the Coulomb contribution, we exploit the linearity of the Poisson equation, and divide the total crystal charge density into localized (corelike) and nonlocalized (valence-like) contributions. The potential arising from the localized piece is computed by direct one-dimensional integration, and the potential from the nonlocalized contribution is calculated by a fast Fourier-transform algorithm.

The bulk diamond calculation of Ref. 13 was performed with a basis set consisting of six  $s$ -type, five  $p$ -type, and one  $d$ -type function, denoted as C(6/5/1), resulting in 26 functions per atom. For the 54-atom supercell of the present work, this would give Hamiltonian matrices of order 1500, much larger than is practical or even necessary. In the interest of a smaller basis set, we have recalculated the diamond band structure using a C(4/3/0) basis set. The adequacy of this smaller basis (13 functions per atom) is demonstrated in Table II by comparing several important features of the eigenvalue spectrum with those given by larger basis sets. Relative to the larger basis set, the C(4/3/0) basis gives self-consistent energies to within 0.05 eV of the fully con-

TABLE II. Bulk diamond band structure, computed with basis sets of various size. For the present calculations, the C(5/4/0) basis was used for the eight- and 16-atom supercells, and the C(4/3/0) basis set for the 54-atom supercell. For all three supercells, the N basis set was N(6/5/0). All energies are in eV.

Basis set	C(6/5/0)	C(5/4/0)	C(4/3/0)	C(3/2/0)
Indirect gap	4.26	4.29	4.31	4.41
Direct gap	5.51	5.52	5.54	5.56
VB width	21.47	21.47	21.46	21.35

verged results. For all three supercells, the nitrogen basis was N(6/5/0). Brillouin-zone sampling was performed with four and two special  $\mathbf{k}$  points in an irreducible wedge of the zone, for the eight- and 16-atom unit cells, respectively. For the 54-atom unit cell, the  $\Gamma$  point alone was used.

### III. RESULTS AND DISCUSSION

We begin by describing the features of the electronic spectrum common to all three supercells, then proceed to discuss the issue of convergence with respect to supercell size. (All relevant numerical results are tabulated in Table III.) The nitrogen impurity introduces two states of interest, the bonding and antibonding combinations of the N  $2s$  orbitals mixed with the C dangling-bond orbitals of  $A_1$  symmetry. Both of the resulting eigenstates have  $A_1$  symmetry. The lower-energy state, split off from the bottom of the valence band (VB), is referred to as the “hyperdeep” state; the higher-energy state falls in the diamond fundamental gap. (Two other eigenstates, the bonding and antibonding combinations of N  $2p$  and C  $T_2$  dangling-bond orbitals, will not be discussed in this work.) The density of states (DOS) for the 54-atom supercell is shown in Fig. 1, in which the hyperdeep level is cleanly split off, and the gap state appears as a shoulder on the low-energy side of the diamond CB.

The centroid of the hyperdeep state falls at  $-21.9$  eV (all energy levels are relative to the VB maximum), just below the bottom of the diamond VB. For a state so energetically deep, it is perhaps surprising that the resulting bandwidth is 3.1, 1.4, and 0.4 eV for the eight-, 16-, and

54-atom supercells, respectively. The charge density from this state is shown in Fig. 2, and clearly shows a substantial admixture of C dangling-bond orbitals.

The gap state is substantially less localized, as can be seen from the charge-density contour plot in Fig. 3. The band centroid is located at 5.6, 4.8, and 4.4 eV for the eight-, 16-, and 54-atom supercells, respectively. The associated bandwidths are quite large: 3.9, 2.5, and 1.6 eV, respectively. While these values may strike one as abnormally large, they are quite comparable to an analogous calculation for a vacancy in silicon, also using the same 54-atom supercell, in which a gap state with a bandwidth of 1.2 eV was found.<sup>15</sup> Taking the calculated LDA value for the diamond indirect gap (from Table II) as 4.2 eV, this implies that the centroid of the gap state falls above the CB minimum. As a result, estimating the position of this level *within* the gap becomes somewhat problematic. However, despite the strong dependence of the gap-state *centroid*, the *minimum* of this band state shows a much weaker dependence, with respective supercell values of 3.1, 3.3, and 3.4 eV. Clearly, a large part of the dispersion of this state arises through interaction with diamond CB states; the lower-energy portion of the band is sufficiently far from the CB edge to make it significantly more stable with respect to supercell size.

In the limit of infinite impurity separation,  $D \rightarrow \infty$ , the bandwidth must go to zero, and hence both the centroid and the minimum of this gap-state band must tend toward the same single energy level. We assume that the centroid and the minimum both depend on  $D$  through the relation

$$E(D) = E(\infty) + E_\beta \exp(-\beta D), \quad (2)$$

TABLE III. Major features of the self-consistent electronic structure for the  $C_{n-1}:N$  impurity system, resulting from supercells with  $n = 8, 16,$  and  $54$  atoms. The values in the last column are extrapolated to the isolated impurity limit using Eq. (2). All energies are in eV and are referred to the VB maximum.

	$C_7:N$	$C_{15}:N$	$C_{53}:N$	$C_\infty:N$ (extrap.)
Hyperdeep state				
Centroid	21.8	21.9	21.9	21.9
Bandwidth	3.9	2.5	1.6	0
Gap state				
Centroid	5.6	4.8	4.4	4.2
Minimum	3.1	3.3	3.4	3.4
Bandwidth	3.9	2.5	1.6	0

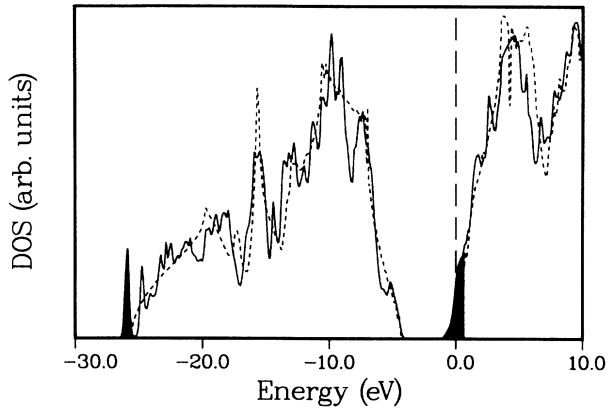


FIG. 1. Density of states (DOS) for the C:N impurity system, as given by the 54-atom supercell  $C_{53}N$ . The two darkened regions are impurity-induced states, the bonding and antibonding combinations of N  $2s$  and C dangling-bond orbitals. The dotted curve is the bulk diamond DOS, shown for reference, and the Fermi level is taken as the zero of energy.

where  $E(\infty)$ ,  $E_\beta$ , and  $\beta$  are free parameters that can be determined exactly from our three supercell results. We find that the centroid extrapolates to  $E(\infty)=4.2$  eV, while the band minimum extrapolates to  $E(\infty)=3.4$  eV. For the reasons outlined in the above paragraph, we take the latter value as our best approximation to the isolated impurity energy level, and we consider the former value

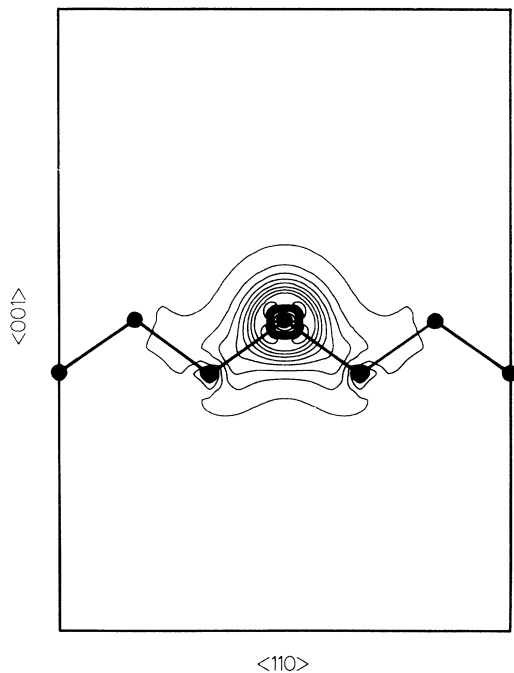


FIG. 2. Charge density from the impurity-induced hyperdeep state at  $-21.9$  eV, relative to the VB maximum, in the 54-atom supercell. The solid circles and lines indicate the positions of C atoms in a bonding chain. Contour lines are separated by  $0.002$  a.u., which is twice the value of the lowest contour.

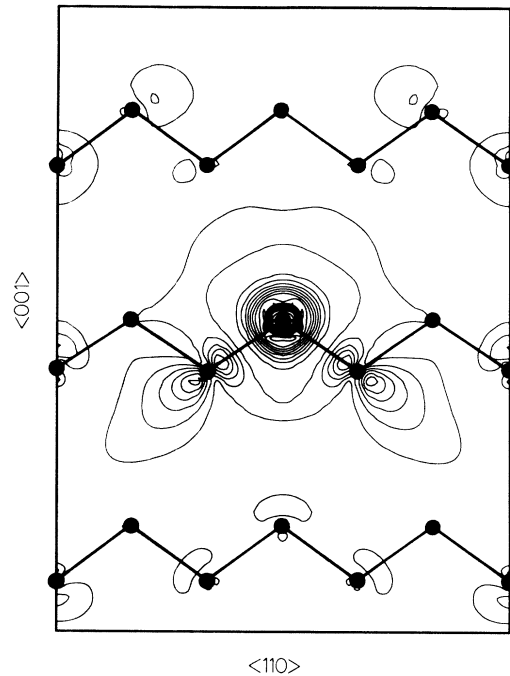


FIG. 3. Charge density from the impurity-induced gap state at  $E_c - 0.8$  eV, where  $E_c$  is the conduction-band edge, in the 54-atom supercell. The solid circles and lines indicate the positions of C atoms in bonding chains. Contour lines are separated by  $0.002$  a.u., which is twice the value of the lowest contour.

to give an approximate handle on the error in this energy-level estimate. Furthermore, since the bottom of the diamond CB is at  $E_c=4.2$  eV, we conclude that the isolated impurity energy level falls at approximately  $E_c - 0.8$  eV, i.e., it is clearly a deep level. While this analysis is by no means the most rigorous possible, it does give a plausible and reasonably accurate description of the relevant energy levels and of the impurity-impurity interaction effects. The dependence of the energy levels on  $D$ , and the energy-level extrapolation to the  $D \rightarrow \infty$  limit, are tabulated in Table III as well as illustrated schematically in Fig. 4.

Our extrapolated gap-state level of  $E_c - 0.8$  eV is in excellent agreement with the LDA value of  $E_c - 0.75$  eV found by Jackson *et al.*,<sup>8</sup> who used a finite cluster and Gaussian orbital methods similar to ours, as well as a Gaussian basis set identical to ours. The 32-atom supercell calculations of Kajihara *et al.*,<sup>9</sup> using a soft-core C pseudopotential, gave a somewhat deeper level at  $E_c - 1.2$  eV. Since those authors did not quote a bandwidth for this state, the degree of impurity-impurity interaction is unknown, and it is difficult to compare this result directly to ours. Direct comparison with the energy-level result of Bachelet *et al.* ( $E_c - 0.15$  eV) is also not possible, since those authors used a simple self-energy correction to account for the well-known deficiency of the LDA, which leads to an underestimate of insulator band gaps by typically 30–50%. The effect of this correction on the diamond band structure is, by construc-

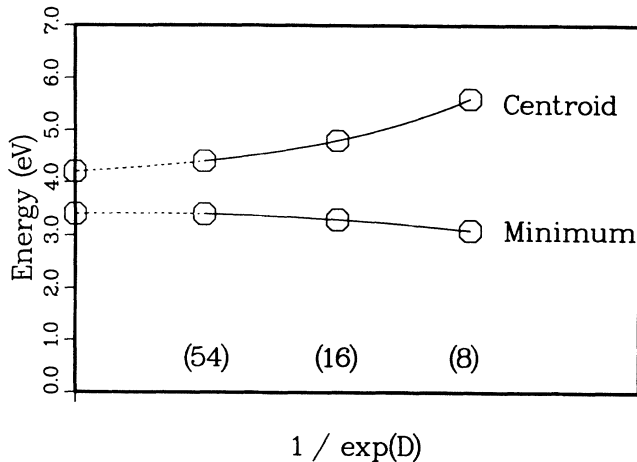


FIG. 4. The band centroid and minimum for the gap state shown in Fig. 3 as a function of impurity-impurity separation  $D$ . An extrapolation to infinite separation (the isolated impurity limit) is given by Eq. (2). The scaling of the abscissa is arbitrary, and is chosen for illustrative purposes only.

tion, to shift rigidly all the conduction bands up in energy by 1.7 eV, so as to produce better agreement with the experimentally measured direct gap of 7.4 eV. The precise effect of this shift on the impurity-induced gap state is not clear.

Experimentally, the N impurity level is found at  $E_c - 1.7$  eV.<sup>16</sup> Although the finding of a deep level is in qualitative agreement with our results, close quantitative agreement is lacking. This is not surprising, however, in light of the problems that the LDA has in predicting energy differences between occupied and unoccupied states. An alternative means of addressing the LDA self-energy problem is the self-interaction correction<sup>17</sup> (SIC), a self-consistent, variationally based method which has been used with great success by a number of workers in atomic,<sup>18,19</sup> molecular,<sup>20</sup> and bulk systems,<sup>21,22</sup> as well as for transition-metal impurities in alkali-halide host crystals.<sup>23–25</sup> In the uncorrected version of the LDA, a given electron (in, say, an isolated atom) experiences a Coulomb potential due to all the electrons in the atom, *including itself*. In Hartree-Fock theory, this “self-Coulomb” term is identically cancelled by a corresponding “self-exchange” term; in the LDA, the use of an approximate exchange (or exchange-correlation) functional renders the cancellation inexact. The residue from this partial cancellation is referred to as “self-interaction,” and has the effect of artificially raising the energies of all the occupied states, relative to the unoccupied states. (This is the origin of the LDA underestimate both of atomic ionization energies and crystalline insulator band gaps, although the latter problem is more often formulated in terms of the derivative discontinuity in the exchange-correlation functional.<sup>26,27</sup>) The essential idea of the SIC is to return to the usual LDA total-energy functional, and append an additional term that removes, on an orbital-by-orbital basis, much of the self-interaction

energy. Application of the usual variational principle then leads to a modified set of Schrödinger-like equations, different from the usual LDA equations only by the addition of a SIC term to the effective one-electron potential. The self-consistent solutions to these equations are generally characterized by occupied states with energies lower than their LDA counterparts, and unoccupied states with energies very little affected (this is in contrast to the Green’s-function self-energy correction mentioned above, which shifts *only* the conduction bands). Although the SIC has not, to our knowledge, been applied to diamond, experience with ionic insulators<sup>22</sup> shows that the SIC generally overcorrects the LDA band gap by amounts ranging from 0–20 %; there is no reason to expect qualitatively different behavior for diamond. Clearly, the result of applying the SIC to the present C:N supercells would be to lower all the occupied bands, resulting in a still deeper defect level, relative to the CB edge. Hence, the agreement between the present results and experiment would be likely to improve somewhat. The same arguments apply to the purely LDA results of Jackson *et al.*<sup>8</sup> and of Kajihara *et al.*<sup>9</sup> Although quantitative comparison of our result with that of Bachelet *et al.*<sup>4</sup> is still not possible, there persists an unresolved qualitative discrepancy between their finding of a shallow level, and our finding of a deep level.

We turn now to two related issues: the degree of localization of the impurity wave function, and the computational adequacy of the supercells in mimicking the isolated impurity. In Fig. 5 we show, for the 54-atom supercell, the valence charge density spanning two adjacent cells. The additional electron introduced by the N impurity is clearly evident in the center of the cell. Diamond bonding chains, with their characteristic double-humped charge accumulations, run zig-zag along the top and bottom of the cells, and are completely undistorted from their appearance in the bulk. The bonding chain

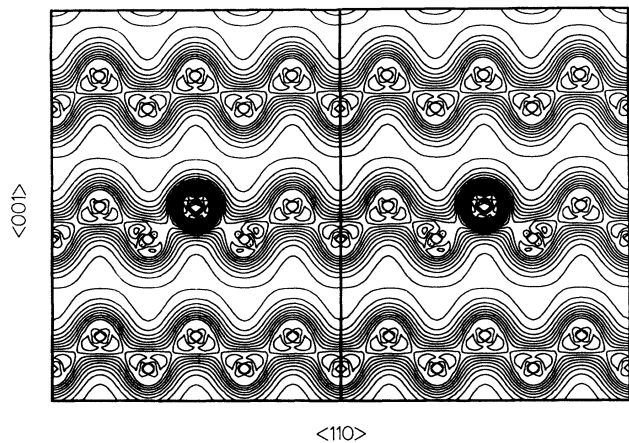


FIG. 5. Valence charge density for the supercell  $C_{53}N$ , spanning two adjacent cells. Note that the disruption of the C bonding chains is almost completely confined to the N atom and its four nearest-neighbor C atoms (two of which lie in the plane of the plot). The contour lines are separated by 0.025 a.u., which is also the value of the lowest contour.

that runs through the middle of the cell is badly distorted only at the first-nearest-neighbor C sites: the bonding lobe that would have been directed toward the central atom in the cell is missing, and the excess charge has contributed to a strengthened bond between the first- and second-nearest-neighbor C atoms. Continuing along this chain, the density around the second-nearest-neighbor C atoms shows only very slight perturbation from its nominal appearance, and the third-nearest-neighbor density (at the edge of the cell) is completely bulklike in appearance. On the basis of such a picture, one might be tempted to conclude that the 54-atom supercell is sufficiently large to mimic the isolated impurity. The results for electronic structure, described in the preceding paragraphs, demonstrate that this conclusion may not be tenable, since perturbations to individual states extend further than do perturbations to the total electronic density. We now offer further evidence to suggest that even greater caution may be warranted when using supercell methods.

One useful way to measure wave-function localization is to integrate the associated charge density enclosed by some fixed volume. We have followed this approach, taking the volume to be given by the innermost five atoms in the unit cell, i.e., the N atom and four nearest-neighbor C atoms, and then integrating the charge density from the (singly occupied) impurity-induced gap state. Three inequivalent integration schemes were used: (i) the charge enclosed by the innermost five touching "muffin-tin" spheres, as a fraction of the total charge enclosed by all such spheres (roughly half an electron); (ii) the total charge, on a dense cubic mesh, from the points that are closest to one of the innermost five atoms; (iii) the radially integrated  $l=0$  component of the density, computed on a spherical mesh centered on the N atom, integrated to a distance midway between the first- and second-

nearest-neighbor shells. This procedure was carried out for all three supercells, with results as displayed in Fig. 6. Although the three different schemes give slightly different results, the overall trend is clear. There is a strong dependence of the integrated charge on supercell size, with averaged charges of 0.87, 0.70, and 0.45 electrons for the eight-, 16-, and 54-atom supercells, respectively. Presumably, the larger values are the result of overlap of tails from neighboring cells, and thus provide a direct measure of supercell adequacy. Moreover, there is no indication that the result for the 54-atom supercell is converged with respect to supercell size, although we note the fair agreement of our 54-atom supercell result with the embedded cluster result of 0.60 electrons found by Bachelet *et al.*<sup>4</sup>

The striking contrast between the total valence density, which appears to effectively shield the impurity after one or, at most, two shells, and the impurity wave-function density, which in this case has a very extensive tail, is a well-known effect.<sup>4</sup> The Hamiltonian depends only on the *total* charge density, and hence is less sensitive to the long-ranged tails of individual states than the above localization analysis might suggest. Indeed, part of the impurity shielding arises from other occupied states with similar spatial extent, whose long-range tails effectively cancel the impurity wave-function tail. Although this cancellation accounts for the relative stability of the impurity wave-function eigenvalues (with respect to supercell size), properties that depend on features of the *individual* impurity states (such as impurity-impurity overlap) will be significantly less reliable.

#### IV. CONCLUDING REMARKS

We have performed first-principles, local-density-approximation calculations for cubic diamond with a substitutional N impurity, using supercells of eight, 16, and 54 atoms. Two impurity-induced states, both with  $A_1$  symmetry, were studied. A hyperdeep level appears at  $-21.9$  eV, relative to the VB maximum, and a deep level appears in the diamond fundamental gap at  $E_c - 0.8$  eV, where  $E_c$  is the CB edge. This latter result is extrapolated, from the sequence of levels given by the three supercells, to the isolated impurity limit. Examination of the charge density from the impurity wave function leads to the conclusion that the wave function from a relatively deep state may extend considerably further from the impurity site than might have been expected. Thus, while energy levels may be predicted from the present supercell studies with confidence, properties that depend on individual wave functions will be more strongly influenced by supercell effects.

There may, however, be situations where the long range of the disturbance of wave functions has important consequences. Such behavior may be observed in magnetic multilayers. Several recent studies have shown that the magnetic coupling between layers of ferromagnetic metals, separated by nonmagnetic "spacing" metal layers, extends to several nanometers of the spacer material; ex-

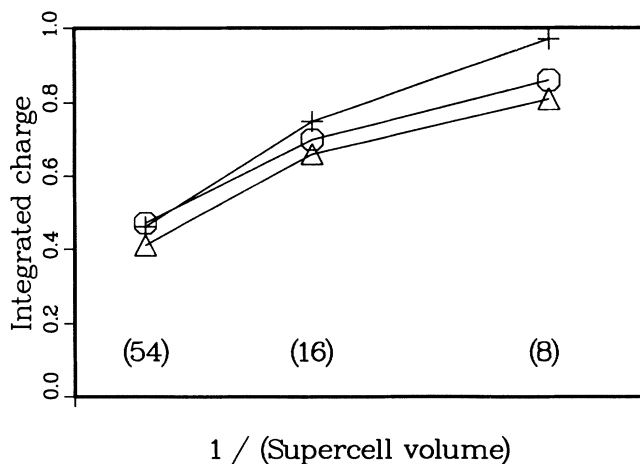


FIG. 6. Integrated charge on the innermost five atoms as a function of impurity-impurity separation  $D$ . The results denoted by circles, triangles, and crosses correspond to the three inequivalent integration schemes (i), (ii), and (iii), respectively (see text). The scaling of the abscissa is arbitrary, and is chosen for illustrative purposes only.

amples are Fe/Cr,<sup>28</sup> Fe/Cu,<sup>29</sup> and Co/Ru.<sup>30</sup> From self-consistent calculations, it seems clear that perturbations in the charge density and spin density decay rapidly (within a few screening lengths, i.e., a few angstroms) away from an isolated interface between two metals, making the observed long-range coupling somewhat mysterious. Our results raise the possibility that the presence of two neighboring interfaces may result in interference effects between individual wave functions, and hence in longer-range coupling (i.e., through thicker spacing layers) than one would predict on the basis of direct coupling via the spin densities of isolated interfaces.

#### ACKNOWLEDGMENTS

We have had many discussions with K. A. Jackson and M. R. Pederson concerning various aspects of their cluster work on the nitrogen impurity problem. One of us (S.E.) acknowledges generous support from the National Research Council. This work was supported by the Innovative Science and Technology Program of the Strategic Defense Initiative Office, administered through the Office of Naval Research. Calculations were performed on the IBM 3090 at the Cornell National Supercomputing Facility.

\*Present address: Department of Physics, University of Pennsylvania, Philadelphia, PA 19104-6396.

- <sup>1</sup>S. C. Erwin and W. E. Pickett, in *Atomic Scale Calculations of Structure in Materials*, edited by M. S. Daw and M. Schlüter (Materials Research Society, Pittsburgh, 1990); W. E. Pickett and S. C. Erwin, in *Diamond, Boron Nitride, Silicon Carbide, and Related Wide-Bandgap Semiconductors*, edited by J. T. Glass, R. F. Messier, and N. Fujimori (Materials Research Society, Pittsburgh, 1990); Phys. Rev. B **41**, 9756 (1990).
- <sup>2</sup>M. R. Pederson, K. A. Jackson, and W. E. Pickett, in *Diamond, Boron Nitride, Silicon Carbide, and Related Wide-Bandgap Semiconductors*, edited by J. T. Glass, R. F. Messier, and N. Fujimori (Materials Research Society, Pittsburgh, 1990).
- <sup>3</sup>M. Astier, N. Pottier, and J. C. Bourgoin, Phys. Rev. B **19**, 5265 (1979).
- <sup>4</sup>G. B. Bachelet, G. A. Baraff, and M. Schlüter, Phys. Rev. B **24**, 4736 (1981).
- <sup>5</sup>R. P. Messmer and P. A. Schultz, Solid State Commun. **52**, 563 (1984); P. A. Schultz and R. P. Messmer, Phys. Rev. B **34**, 2532 (1986).
- <sup>6</sup>R. P. Messmer (private communication).
- <sup>7</sup>N. Sahoo, K. C. Mishra, M. van Rossum, and T. P. Das, Hyperfine Interact. **35**, 701 (1987).
- <sup>8</sup>K. A. Jackson, M. R. Pederson, and J. G. Harrison, Phys. Rev. B **41**, 12 641 (1990).
- <sup>9</sup>S. A. Kajihara, A. Antonelli, and J. Bernholc, in *Diamond, Boron Nitride, Silicon Carbide, and Related Wide-Bandgap Semiconductors*, edited by J. T. Glass, R. F. Messier, and N. Fujimori (Materials Research Society, Pittsburgh, 1990).
- <sup>10</sup>M. Lannoo, Phys. Rev. B **25**, 2987 (1982).
- <sup>11</sup>S. J. Sferco and M. C. G. Passeggi, Solid State Commun. **62**, 517 (1987).
- <sup>12</sup>L. Hedin and B. I. Lundqvist, J. Phys. C **4**, 2064 (1971).
- <sup>13</sup>S. C. Erwin, M. R. Pederson, and W. E. Pickett, Phys. Rev. B **41**, 10437 (1990).
- <sup>14</sup>R. D. Chaney, T. K. Tung, C. C. Lin, and E. E. Lafon, J. Chem. Phys. **52**, 361 (1970).
- <sup>15</sup>S. G. Louie, M. Schlüter, J. R. Chelikowsky, and M. L. Cohen, Phys. Rev. B **13**, 1654 (1976).
- <sup>16</sup>R. G. Farrer, Solid State Commun. **7**, 685 (1969).
- <sup>17</sup>J. P. Perdew and A. Zunger, Phys. Rev. B **23**, 5048 (1981).
- <sup>18</sup>J. G. Harrison, J. Chem. Phys. **78**, 4562 (1983).
- <sup>19</sup>M. R. Pederson and C. C. Lin, J. Chem. Phys. **88**, 1807 (1988).
- <sup>20</sup>M. R. Pederson, R. A. Heaton, and C. C. Lin, J. Chem. Phys. **82**, 2688 (1985).
- <sup>21</sup>R. A. Heaton, J. G. Harrison, and C. C. Lin, Phys. Rev. B **28**, 5992 (1983); R. A. Heaton and C. C. Lin, J. Phys. C **17**, 1853 (1984).
- <sup>22</sup>S. C. Erwin and C. C. Lin, J. Phys. C **21**, 4285 (1988).
- <sup>23</sup>R. A. Heaton, J. G. Harrison, and C. C. Lin, Phys. Rev. B **31**, 1077 (1985).
- <sup>24</sup>K. A. Jackson and C. C. Lin, Phys. Rev. B **38**, 12171 (1988); **41**, 947 (1990).
- <sup>25</sup>S. C. Erwin and C. C. Lin, Phys. Rev. B **40**, 1892 (1989).
- <sup>26</sup>J. P. Perdew and M. Levy, Phys. Rev. Lett. **51**, 1884 (1983).
- <sup>27</sup>L. J. Sham and M. Schlüter, Phys. Rev. Lett. **51**, 1888 (1983).
- <sup>28</sup>J. J. Krebs, P. Lubitz, A. Chaiken, and G. A. Prins, Phys. Rev. Lett. **63**, 1645 (1989).
- <sup>29</sup>B. Heinrich *et al.*, Phys. Rev. Lett. **64**, 673 (1990).
- <sup>30</sup>S. S. Parkin, N. More, and K. P. Roche, Phys. Rev. Lett. **64**, 2304 (1990).